Carbon Black Nanoparticles Impair Acetylation of Aromatic Amine Carcinogens through Inactivation of Arylamine *N*-Acetyltransferase Enzymes

Elodie Sanfins,[†] Julien Dairou,[†] Salik Hussain,[†] Florent Busi,[†] Alain F. Chaffotte,[§] Fernando Rodrigues-Lima,[†] and Jean-Marie Dupret[†,*]

[†]Univ Paris Diderot, Sorbonne Paris Cité, Unité de Biologie Fonctionnelle et Adaptative, CNRS EAC4413, 75013, Paris, France, and [§]Institut Pasteur, Unité de RMN des Biomolécules, 75015, Paris, France

ABSTRACT Carbon black nanoparticles (CB NPs) and their respirable aggregates/agglomerates are classified as possibly carcinogenic to humans. In certain industrial work settings, CB NPs coexist with aromatic amines (AA), which comprise a major class of human carcinogens. It is therefore crucial to characterize the interactions of CB NPs with AA-metabolizing enzymes. Here, we report molecular and cellular evidence that CB NPs interfere with the enzymatic acetylation of carcinogenic AA by rapidly binding to arylamine *N*-acetyltransferase (NAT), the major AA-metabolizing enzyme. Kinetic and biophysical analyses showed that this interaction leads to protein conformational changes and an irreversible loss of enzyme activity. In addition, our data showed that exposure to CB NPs altered the acetylation of 2-aminofluorene in intact lung Clara cells by impairing the endogenous NAT-dependent pathway. This process may represent an additional mechanism that contributes to the carcinogenicity of inhaled CB NPs. Our results add to recent data suggesting that major xenobiotic detoxification pathways may be altered by certain NPs and that this can result in potentially harmful pharmacological and toxicological effects.

KEYWORDS: lung Clara cells · xenobiotic metabolism · irreversible inhibition · enzyme · protein conformation

A dramatic increase in the industrial production and use of nanoparticles (NPs) has taken place over the past decades, yet the potential toxic effects of NPs are far from being clearly understood.[1] Carbon black nanoparticles (CB NPs) are widely used in industrial production.[2] These particles are most often produced by controlled incomplete combustion or thermal decomposition of hydrocarbons. The expected increase in worldwide demand for CB NPs (for example in the production of tires, rubbers, plastics and printing inks) and their prevalence in the environment due to large-scale production requires that we understand how these particles interact with biological processes.

CB NPs and their respirable aggregates/agglomerates are classified as possibly carcinogenic to humans (group 2B).[3,4] Of primary concern is the possible synergy between CB NPs and toxic pollutants which themselves present particle-induced toxicity. Indeed, approximately 90% of CB is used in rubber applications,[5,6] and CB along with aromatic amines (AA) are major raw materials for automobile tire manufacturing.[7] AA represent one of the most important classes of occupational or environmental pollutants. They are a common byproduct of chemical manufacturing (dyestuffs, pesticides, rubbers, or pharmaceuticals), coal and gasoline combustion, and pyrolysis reactions. Many AA are toxic to most living organisms due to their genotoxic or cytotoxic properties.[8] AA account for 12% of the chemicals either known to be or strongly suspected to be carcinogenic in humans.[9] Exposure assessment studies have shown that workers employed in the rubber manufacturing industry are exposed to numerous airborne xenobiotics, including AA, which have been shown to be carcinogenic and/or mutagenic.[10] Since CB NPs and AA compounds coexist in such industrial work settings, the possibility that carcinogenic AA metabolism in cells is modified by CB NPs needs to be explored.

Most of the observed biological effects of NPs are likely due to their interactions with proteins,[11] including enzymes involved in various biological pathways.[12] To gain a better understanding of the toxicological effects of CB NPs, including their carcinogenicity, it is crucial to characterize their interactions with xenobiotic/carcinogen-metabolizing enzymes (XME). NPs have been reported to

* Address correspondence to jean-marie.dupret@univ-paris-diderot.fr.

Received for review December 20, 2010 and accepted April 28, 2011.

Published online April 28, 2011
10.1021/nn103534d

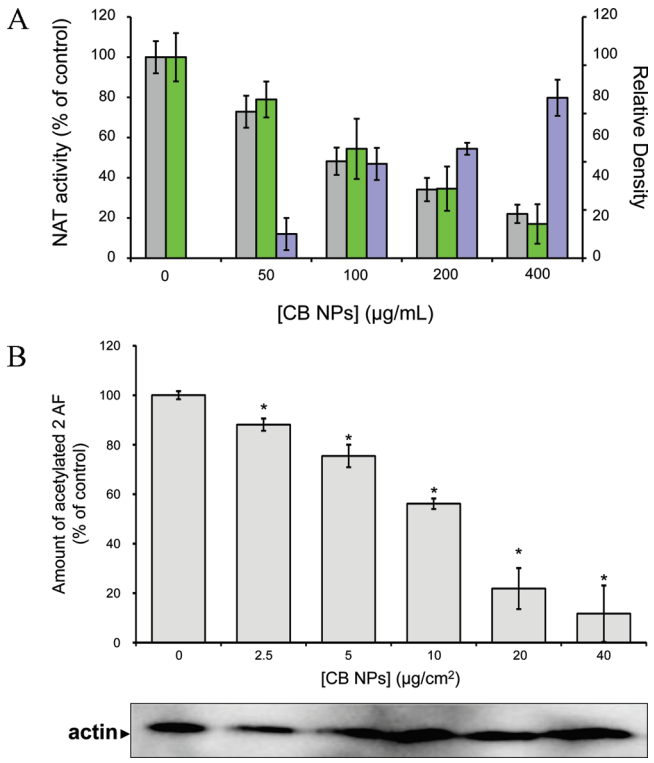

Figure 1. Inactivation of endogenous NAT activity in Clara cells and impairment of 2-AF acetylation by cultured Clara cells upon exposure to CB NPs. (A) Cell extracts (15 mg/mL protein concentration) were exposed to CB NPs (50−400 μg/mL) at 37 °C for 30 min. Extracts exposed only to PBS were used as controls. Residual NAT activity in cell extracts was assessed by HPLC using 2-AF as a substrate (gray bars). After centrifugation, the relative amounts (relative density) of NAT in the supernatant (green bar) and in the CB NP-pellets (blue bar) were measured in western-blots using the Multigauge software (FujiFilm, Japan). The 100% value for the CB NP-pellets (blue bars) corresponds to the amount of NAT enzyme present in extract (15 mg/mL total protein) not incubated with CB NPs. Error bars indicate the SD values. (B) Cells in 6-well plates were exposed to different concentrations of CB NPs for 2 h. Following CB NP treatment, cells were washed and grown in fresh culture medium in the presence of 500 μM of 2-AF. The amount of acetylated-2-AF in culture medium was quantified by HPLC. The maximal amount of acetylated 2-AF generated in 1 h (100%) was equivalent to 320 pmol. Error bars indicate the SD values (∗, $p < 0.05$). In addition to cell counting, antiactin western-blots were used to ascertain whether the numbers of cells in the wells at the beginning of the experiment and at the end were the same (lower panel).

exert different types of effects on enzymes, including catalytic activation, stabilization, or inactivation.[13−16] With respect to carcinogen-metabolizing enzymes, recent studies have shown that certain NPs, such as those consisting of polystyrene[17] or silver,[18] can inhibit the activity of an important class of XME, the cytochrome P450 isoenzymes.

Arylamine *N*-acetyltransferases (NAT) are XME which are particularly relevant for assessing the effects of CB NPs on AA metabolism. Indeed, NAT catalyze the acetyl-CoA-dependent *N*- and/or *O*-acetylation of AA and their *N*-hydroxylated metabolites.[19] The *N*-acetylation reaction leads to the detoxification of AA through the production of chemically stable arylacetamides. Conversely, *O*-acetylation of hydroxylamines leads to faster rate of production of reactive electrophilic compounds. Therefore, NAT-dependent acetylation of AA is a major biotransformation pathway which can have pharmacological and toxicological consequences. In particular, variations in NAT activity have long been associated with susceptibility to different cancers, some of which are also related to AA exposure.[20]

Here we report molecular and cellular evidence that CB NPs interfere with the enzymatic acetylation of carcinogenic AA by rapidly binding to NAT enzymes. Kinetic and biophysical analyses showed that this interaction leads to protein conformational changes and irreversible losses in enzyme activity.

RESULTS AND DISCUSSION

To investigate the effects of CB NPs on the NAT-dependent biotransformation of AA, we used well-characterized commercially available CB NPs (FW2) from Degussa. Supplementary Table 1 (see Supporting Information) summarizes their key physicochemical characteristics (diameter, surface area, zeta potentials, and hydrodynamic diameters of the suspended particles in water, PBS, and DMEM F-12). These CB NPs are carbonaceous NPs that possess surface sites containing mono- and dicarboxylic acids, as well as carbonyl groups of aldehydes and ketones.[21] The aggregate size is not equal to the primary particle size (13 nm) and the mean hydrodynamic diameter of the aggregates was close to 300 nm. Similar levels of CB NP aggregation

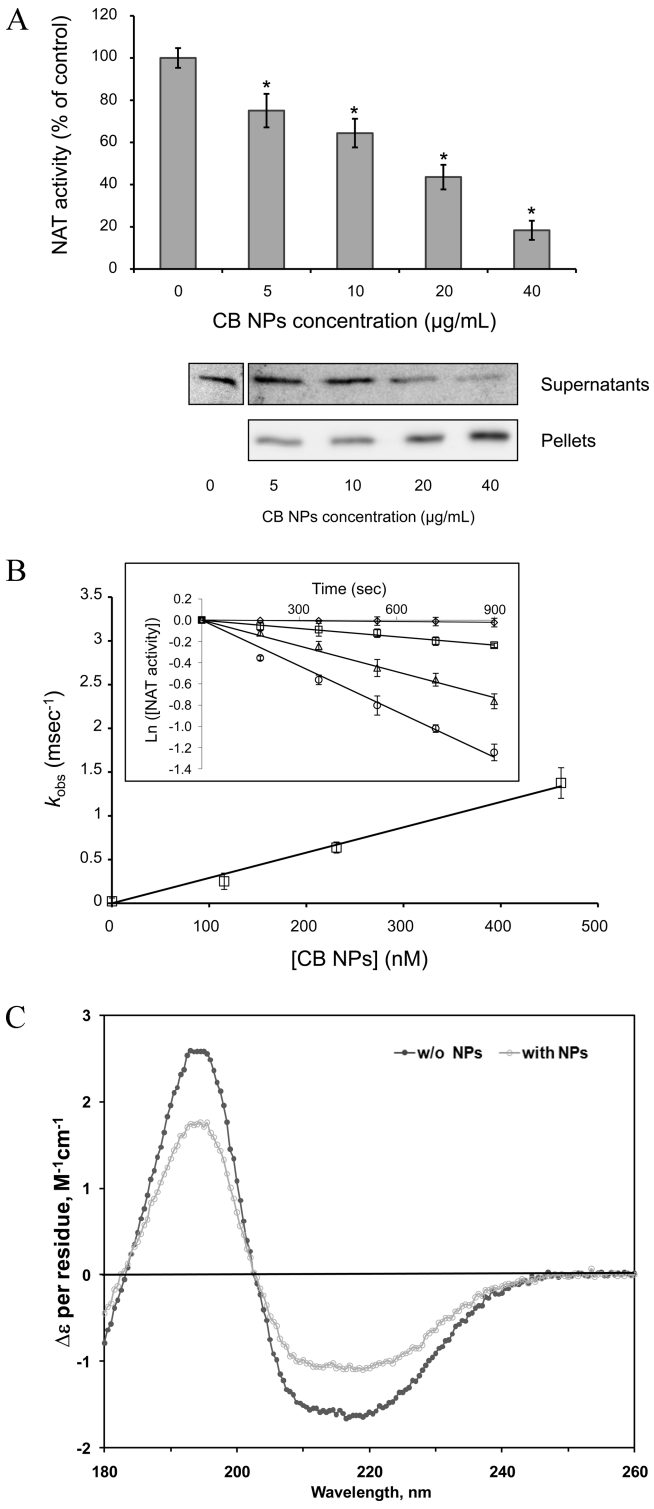

Figure 2. Effect of CB NPs on human recombinant NAT1. (A) NAT1 was incubated with different concentrations of CB NPs (5−40 μg/mL) at 37 °C for 30 min and then residual activity was measured using PAS as substrate (gray bars). NAT1 exposed only to PBS was used as control. Error bars indicate the SD values. After centrifugation (30 min at 100 000 *g*), supernatants and NP-pellets were analyzed by Western blot using an anti-NAT antibody. (B) NAT1 (30 nM, final concentration) was treated with CB NPs (at final concentrations between 115 and 460 nM corresponding to 10−40 μg/mL) at 37 °C and the residual activity was assayed with PAS in aliquots taken at various times. Inset: plots of the natural logarithm of percent residual activity *versus* time. The apparent first-order inactivation constants (k_{obs}) were calculated from linear regressions. The apparent second-order rate constant (k_{inact}^{app}) was determined using linear regression (k_{obs} *versus* CB NPs concentration). Error bars indicate the SD values (C) Far UV spectra of human NAT1 (3 μM) in the presence (gray line) and in the absence (black line) of CB NPs (40 μg/mL).

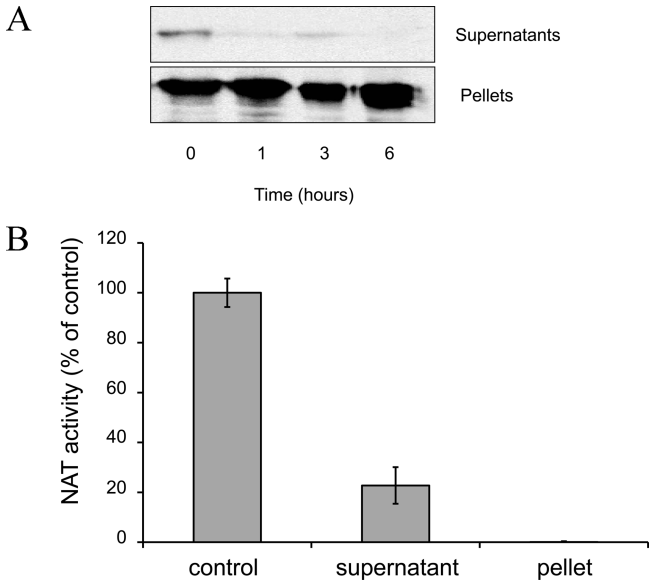

Figure 3. Time course analysis of CB NP-bound NAT1 and impairment of NAT activity. (A) CB NPs (40 μg/mL) were preincubated with purified NAT1 enzyme (100 μg/mL) in 1 mL of PBS for 30 min at 37 °C to generate CB NP-NAT1 conjugates. After ultracentrifugation (100 000 *g*, 30 min, 4 °C), CB NP pellets were recovered in 1 mL of PBS and incubated at 37 °C. At different time points (0, 1, 3, and 6 h), 100 μL of the mixture was taken and submitted to ultracentrifugation. The supernatant was saved for further analysis. The CB NP pellets were washed once with PBS, and bound NAT1 enzyme was eluted from the pellets in 20 μL of 4X SDS-sample buffer. Supernatants (50 μL) and eluates (10 μL) were analyzed by SDS-PAGE and Western blotting (see Methods). (B) CB NPs (40 μg/mL) were preincubated with purified NAT1 enzyme (100 μg/mL) in 1 mL of PBS for 30 min at 37 °C to generate CB NP-NAT1 conjugates. After ultracentrifugation (100 000 *g*, 30 min, 4 °C), the supernatant was saved to determine NAT enzyme activity (see Methods). The CB NP pellet was resuspended in 1 mL of PBS and ultracentrifuged again. CB NP-NAT1 conjugates were resuspended in 100 μL of NAT assay buffer (PBS containing 200 μM PNPA). NAT activity in the mixture was assayed at 37 °C as described in the Methods using PAS as substrate. NAT1 enzyme (100 μg/mL) in 1 mL of PBS was used as control.

have been reported previously.[22,23] We have observed that these CB NPs are internalized very rapidly by cell monolayers (requiring exposures of as little as 30 min) and the internalized amount remains nearly constant between 2 and 24 h.[24] Moreover, these CB NPs have been shown to exert biological effects in lung and renal epithelial cells.[22,23]

Lung epithelial cells are known to be a primary defense against pulmonary toxicants and represent possible targets in lung carcinogenesis.[25] We reported previously that functional human NAT1 (or its murine ortholog, NAT2) is present in different types of pulmonary epithelial cells, such as Clara cells or type II alveolar cells. These data indicated that inhaled AA may undergo NAT-dependent biotransformation in lung epithelium. Clara cells represent up to 80% of the epithelial cell population of the distal airways[26] and have been shown to be involved in the biotransformation of environmental chemicals.[27−29] The role of Clara cells in the carcinogenesis of pulmonary epithelia is also well documented.[26] We therefore assessed the sensitivity of NAT enzyme to CB NPs by exposing extracts from cultured Clara cells to different concentrations of CB NPs (Figure 1). Exposure of Clara cell extract to CB NPs (50 to 400 μg/mL) caused significant concentration-dependent inactivation of the endogenous NAT enzyme (Figure 1A). CB NPs at 95 μg/mL inactivated 50% of cellular NAT. After centrifuging the extract samples to sediment the CB NPs, immunoblot analysis of the extract supernatants showed a CB NP dose-dependent decrease in immunoreactive NAT enzyme which paralleled the losses observed in the enzyme activity assay. Immunoblot analysis of the pellet samples showed that the loss of immunoreactive NAT enzyme from the supernatants was mainly due to its accumulation in the CB NP-pellets (Figure 1A). These data suggest that a direct interaction between CB NPs and the endogenous NAT enzyme led to its functional impairment. To confirm this hypothesis, we investigated the ability of CB NPs to impair the cellular *N*-acetylation of 2-aminofluorene (2-AF, a prototypic carcinogenic substrate of NAT) in living cells. We exposed Clara cells to CB NPs for 2 h and subsequently to 2-AF for 1 h. We observed that the amount of acetylated 2-AF in the cell culture medium decreased in a dose-dependent manner, with an IC_{50} of ~10 μg/cm^2 (Figure 1B). Overall, these data indicated that exposure to CB NPs altered 2-AF acetylation in intact lung epithelial cells by impairing the endogenous NAT-dependent pathway. We obtained similar results with A549 cells, a lung alveolar epithelial cell line (data not shown).

Human recombinant NAT1 enzyme was used to investigate the effect of CB NPs on NAT activity at the molecular level. NAT1 enzyme was incubated for 30 min with various concentrations of CB NPs (up to 40 μg/mL).

NAT activity was significantly inhibited by CB NPs in a dose-dependent manner ($IC_{50} \approx 15\ \mu g/mL$) (Figure 2A). After ultracentrifugation, immunoblot analysis of supernatant samples using an anti-NAT antibody showed a CB NP-dose dependent decrease in immunoreactive protein which paralleled the losses observed in the enzyme activity. Immunoblot analysis of pellet samples using the same antibody showed that the losses of immunoreactive enzyme from the supernatants were mainly due to its accumulation in CB NP-pellet (Figure 2A). These results further supported the existence of a direct interaction between CB NPs and NAT1 enzyme. We next carried out a time-course study to analyze the stability of the CB NP-NAT1 conjugates and found that these conjugates remained stable for at least 6 h (Figure 3A).

To gain further insights into the mechanisms by which CB NPs inactivate recombinant NAT1, we performed kinetic analyses. The inhibition was found to obey an irreversible bimolecular process which can be represented by the following equation: $-d[NAT1]/dt = k_{inact} \cdot [NAT1] \cdot [CB\ NPs]$, where [NAT1] is the concentration of active enzyme and k_{inact} is the second-order rate constant. The apparent first order inactivation rate constant ($k_{obs} = k_{inact} \cdot [CB\ NPs]$) was calculated for each CB NPs concentration from the slope of natural log (ln) of the residual activity percentage plotted against time. The second order rate constant was determined from the slope of k_{obs} against CB NP concentration. CB NP molarity values were estimated on the basis of a CB NP diameter of 13 nm. However, due to extensive CB NP aggregation (with a mean hydrodynamic diameter of ~300 nm), the true kinetic constant was likely to be underestimated. Therefore, given the apparent size heterogeneity of the aggregates, it was not possible to calculate k_{inact} more precisely, and it should be considered an apparent constant (k_{inact}^{app}). Nevertheless, the data showed that the enzyme was rapidly and irreversibly inactivated by CB NPs, with an apparent second-order rate constant (k_{inact}^{app}) for enzyme inactivation of $2.90 \times 10^3\ M^{-1} \cdot sec^{-1}$ (Figure 2B). For CB NP aggregates of 300 nm, we estimated a value of $3.30 \times 10^7\ M^{-1} \cdot sec^{-1}$ for k_{inact}^{app}.

Our centrifugation experiments (Figures 1A and 2A) suggested that a direct interaction between CB NPs and the NAT enzyme led to its inactivation. To test whether CB NP-bound NAT1 was inactive, CB NP conjugates were assayed for NAT activity (Figure 3B). These experiments showed that CB NP-NAT1 conjugates were devoid of enzyme activity. To further understand the mechanism underlying the inactivation of NAT1 by CB NPs, we used CD spectroscopy to assess whether the CB NPs were responsible for conformational changes in the enzyme structure. NAT1 far UV spectra were recorded in the absence or presence of CB NPs (40 μg/mL, a concentration that yielded nearly full enzyme inactivation, Figure 2C). The spectrum of

TABLE 1. Analysis of the Composition of the Secondary Structures with or without CB NPs[a]

	α helix (%)	β sheet (%)	other (%)	rmsd
w/o NPs	14	33.6	52.4	0.031
with NPs	6.9	37.9	55.2	0.048

[a] Deconvolution of the CD spectra was carried out using CONTIN software included in CDpro http://lamar.colostate.edu/~sreeram/CDPro/[33] with a database consisting of 42 soluble proteins.

TABLE 2. Effects of Reducing Agents on Recombinant NAT1 Activity in the Presence or Absence of CB NPs (40 μg/mL)[a]

conditions	activity (%)
control	100
NAT1 + CB NPs	4.5 ± 4
NAT1 + CB NPs + GSH (2 mM)	6.1 ± 7
NAT1 + CB NPs + GSH (4 mM)	9.3 ± 5
NAT1 + CB NPs + DTT (1 mM)	22 ± 12
NAT1 + CB NPs + DTT (2 mM)	18 ± 6

[a] The values shown are means of three independent experiments, in which each treatment was performed in quadruplicate. Assays were done with PAS as substrate. Values obtained with GSH and DTT are not statistically different from the value obtained with NAT1+CB NPs (ANOVA followed by Student *t*-test with Bonferroni correction). $p < 0.05$ for NAT1+CB NPs *versus* Control.

NAT1 without CB NPs showed a positive band near 192 nm and a negative band near 220 nm. The addition of CB NPs triggered a decrease of the positive band and an increase of the negative band, which indicated that secondary structures in NAT1 had changed (Figure 2C). The CD spectra were deconvoluted, and the deduced compositions of the secondary structures were analyzed (Table 1). The presence of CB NPs was accompanied by a decrease in the α-helical content (14%−6.9%) and an increase in the β-strand content (33.6%−37.9%). These CD data demonstrated that the secondary structures of NAT1 were sensitive to CB NP binding. Overall, our results suggest that NAT1 helices are destabilized by CB NP binding, which leads to structural changes and subsequent enzyme inactivation.

It has been reported that the CB NPs used in our study (Degussa FW2) are capable of generating reactive oxygen species (ROS) under abiotic conditions.[24,30] These properties are likely due to industrial manufacturing processes (involving a post-treatment with oxidants) which create mono- and dicarboxylic acid groups and carbonyl groups of aldehydes and ketones on the surface of these CB NPs.[21] ROS are generally destructive in nature, and NAT enzymes are well-known to be inactivated by oxidative species.[31] Thus, we investigated whether thiol-reducing agents could protect NAT1 from inactivation by CB NPs. Incubating the enzyme with CB NPs in the presence of high concentrations (1, 2, or 4 mM) of DTT (1,4-dithiothreitol) or GSH (reduced glutathione) afforded no

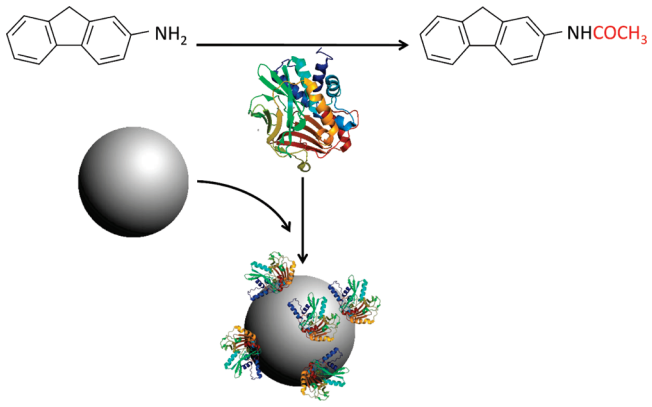

Figure 4. Model showing interaction between CB NPs and the NAT-dependent acetylation pathway.

significant protection against CB NP-mediated NAT1 inactivation (Table 2). We conclude that the ROS intrinsically produced by CB NPs had no significant effect on NAT activity.

Overall, our cellular and mechanistic studies provide evidence that CB NPs can alter the biotransformation of AA carcinogens through the impairment of the NAT-dependent acetylation pathway (Figure 4). This process may represent an additional mechanism that may contribute to the carcinogenicity of inhaled CB NPs. Co-exposure to CB NPs and aromatic chemicals such as AA is a very likely occupational hazard in several industrial work settings.[7] Although the data presented here were obtained using *in vitro* approaches and therefore cannot be inferred directly to *in vivo* studies, our results support the view that major xenobiotic detoxification pathways may be altered by certain NPs, and that this can lead to potentially harmful pharmacological and toxicological effects.[17,18]

METHODS

Materials. FW2 (13 nm) carbon black nanoparticles (CB NPs) were obtained from Evonik Industries/Degussa (Frankfurt, Germany). Details about these NPs are given below. *para*-Aminosalicylic acid (PAS), acetyl (Ac)CoA, 1,4-dithiothreitol (DTT), reduced glutathione (GSH), protease inhibitor cocktail, and nickel agarose resin were obtained from Sigma. The Bradford protein assay kit was supplied by Bio-Rad. All other reagents were purchased from Euromedex unless otherwise noted. Polyclonal antihuman NAT1 (which cross-reacts with murine NAT2) were kindly provided by Pr. Edith Sim (Oxford University, UK).

Stock solutions of CB NPs (2 mg/mL) were prepared in pure water and sonicated 10 min to improve dispersal of particles. The CB NPs used did not bind the aromatic amine substrates used in this study (data not shown).

Production and Purification of Recombinant Human NAT1. *Escherichia coli* BL21 (DE3) cells containing a pET28a-based plasmid were used to produce 6x-HIS tagged NAT1, as described previously.[32] Purified NAT1 was reduced by incubating it with 10 mM DTT for 10 min at 4 °C and dialyzing it against phosphate-buffered saline, pH 7.5 (PBS). Purity was assessed by SDS-PAGE, and protein concentrations were determined using the Bradford reagent following the manufacturer's instructions and bovine serum albumin as a standard.

Activity of recombinant NAT1. NAT1 activity was detected in a total volume of 100 μL. Samples containing recombinant enzyme were first incubated with PAS in PBS at 37 °C for 5 min. PNPA (200 μM) was added to start the reactions. The samples were then incubated for various periods (up to 30 min) at 37 °C and the absorbance was measured every 2 min at 450 nm. All assays were performed in triplicate under initial reaction rate conditions. Enzyme activity is expressed as a percentage of the control. In all reaction mixtures, the final concentration of NAT1 was 30 nM.

Interaction of Recombinant NAT1 with CB NPs. In all subsequent experiments, the final concentration of NAT1 during the incubation steps with the CB NPs was 100 μg/mL (3 μM). The effect of CB NPs on NAT1 activity was assessed by incubating the purified enzyme with various concentrations of CB NPs in PBS for 30 min at 37 °C. Aliquots were then assayed for NAT1 activity. In parallel, aliquots were ultracentrifuged (100 000 *g*, 30 min, 4 °C). The supernatant was saved for further Western blot analysis, and the CB NP pellet was washed with PBS and ultracentrifuged again. NAT1 proteins bound to CB NP pellets were eluted by incubation with 4× SDS-sample buffer and used for Western blot analysis.

Effects of Reducing Agents on CB NP-Dependent Inhibition of Recombinant NAT1. We tested the ability of reducing agents to protect NAT1 from the oxidative effects of CB NPs by coincubating the NAT1 enzyme with CB NPs at 40 μg/mL in presence of high concentrations of GSH or DTT (two ROS scavengers). Upon incubation at 37 °C for 30 min the residual NAT1 activity of the mixture was measured. Control assays were carried out with GSH or DTT in the absence of CB NPs and were found to have no effect on NAT1 enzyme activity (data not shown).

Kinetic Analysis of CB NP-Dependent NAT1 Inactivation. NAT1 (final concentration of 30 nM) was incubated with CB NPs (at final concentrations between 115 and 460 nM) at 37 °C in PBS. At various time intervals, aliquots were removed and assayed for residual activity. The data were fitted to an irreversible pseudo-first-order process (ln [residual activity] = $-k_{obs}t$) where k_{obs} is the first-order inactivation rate constant obtained for each CB NP concentration and t is the time (in seconds). The second-order inactivation rate constant (k_{inact}) was determined from the plot of the k_{obs} values as a function of CB NP concentration as $k_{obs} = k_{inact}$[CB NPs]. KaleidaGraph version 3.5 (Abelbeck/Synergy, Reading, PA) was used for mathematical treatment of the kinetic data.

Circular Dichroism. Circular dichroism measurements were achieved using an Aviv215 spectropolarimeter. Protein samples were exhaustively dialyzed against 10 mM sodium phosphate, pH 7.5. Far-UV CD spectra were acquired from 180 to 260 nm through a cylindrical cell with a 0.02 cm path length. Ellipticity

was recorded at 0.5 nm intervals with an averaging time of 1 s/step. The protein concentration was 960 μg/mL. To minimize the signal-to-noise ratio, five successive scans were averaged and the baseline acquired using dialysis buffer alone under strictly identical conditions was then subtracted. Resulting spectra were then normalized to the protein concentration expressed as the differential molar extinction coefficient ($\Delta\varepsilon$) per residue. Secondary structure predictions were deduced from the normalized spectra using the CDPro package (ref 33, http://lamar.colostate.edu/~sreeram/CDPro/main.html).

SDS-PAGE and Western blotting. The samples containing 4X SDS sample buffer were boiled for 5 min at 95 °C, and the proteins were separated by SDS-PAGE. For Western blotting, proteins were electrotransferred onto a nitrocellulose membrane. The membrane was blocked by incubation with Tris-buffered saline/Tween 20 (TBS) supplemented with 5% nonfat milk powder for 1 h. Antibodies were added (1/20000) and the membrane was incubated for 1 h in TBS. Supersignal reagent (Pierce chemical, Rockford, IL) was used to detect the bound antibodies. The amount of NAT enzyme was quantified in Western blots using Multigauge Software (FujiFilm, Japan).

Cell Culture, Total Cell Extracts, and Exposure to CB NPs. The Clara epithelial cell line[34] was kindly provided by Pr. J. M. Sallenave (Institut Pasteur, Paris, France) and grown in DMEM supplemented with 20% (v/v) FBS. This cell line is well-described as a lung epithelial cell model involved in the biotransformation of xenobiotics in the lung.[29,34] Cells were cultured as monolayers in 35 or 100 mm tissue culture dishes at 37 °C. At confluence, the cells were at a density of 4×10^4 cells/cm^2.

To make whole-cell extracts, confluent monolayers were washed with PBS and scraped into 0.5−1 mL of lysis buffer (PBS, 0.1% Triton X-100) containing protease inhibitors. Extracts were sonicated and centrifuged for 15 min at 13 000 *g*. Supernatants (whole-cell extracts) were removed and their protein concentration determined using the Bradford reagent.

The effect of CB NPs on cellular NAT enzyme activity was assessed by incubating cell extracts (15 mg/mL total protein) to CB NPs (50 to 400 μg/mL) at 37 °C for 30 min with constant shaking. NAT activity in treated cell extracts was measured using 2-AF as a substrate and HPLC to measure product formation. In parallel, aliquots were centrifuged (10 min at 13 000 *g*) to separate NP-bound proteins from unbound proteins. After washes with PBS, NP-bound proteins were eluted with 4× SDS sample buffer.

NAT Activity in Cells Extracts. NAT activity was measured in cell extracts using reverse-phase HPLC as described previously.[35] Samples (50 μL) were first incubated with 2-AF (1 mM, final concentration) in assay buffer (PBS, pH 7.5) at 37 °C for 5 min. AcCoA (1 mM, final concentration) was added and the samples (100 μL, final volume) were incubated at 37 °C for various periods of time (up to 30 min). The reaction was quenched by adding 100 μL of ice-cold acetic acid (15% w/v), and proteins were recovered by centrifugation for 5 min at 12 000 *g*. A 20 μL portion of the supernatant was subjected to C18 reverse-phase HPLC. Both the parent AA compound and its acetylated metabolite were detected and measured. All assays were performed in triplicate under initial reaction rate conditions.

Acetylation of 2-AF by Intact Clara Cells in Culture. Acetylation of 2-AF by endogenous NAT in intact cells was measured by reverse-phase HPLC as described previously.[36] Briefly, after exposure to CB NPs (up to 40 μg/cm^2 corresponding to 100 μg/mL), the confluent monolayers (6-well plates, 10 cm^2 per well, 4×10^5 cells/well, ~100 μg total protein) were washed with PBS and grown in the presence of 500 μM 2-AF in DMEM culture medium in a 37 °C incubator. At different time points (3, 4, 5, and 6 h), aliquots (100 μL) of culture medium were collected and added to 100 μL of ice-cold aqueous acetic acid (15% w/v). Samples were then centrifuged and the amount of acetylated-2-AF was quantified by HPLC analysis. Controls were performed using the same conditions and with cell monolayers not exposed to NPs. Both the parent AA compound and its acetylated metabolite were detected and measured. The appearance of *N*-acetylated AA and the disappearance of the parent AA in the culture medium were found to be linear with time.

Acknowledgment. We thank E. Petit for technical assistance. E.S. is supported by a Ph.D. fellowship from Ministère de l'Enseignement Supérieur et de la Recherche. S.H. is a Ph.D. fellow of Higher Education Commission of Pakistan. We thank R. Karess for reading the manuscript. This work was supported by grants from "la Caisse d'Assurance Maladie des Professions Libérales de Province". We acknowledge the technical platform "BioProfiler-UFLC" for provision of HPLC facilities.

Supporting Information Available: Physicochemical parameters of CB NPs. This material is available free of charge *via* the Internet at http://pubs.acs.org.

REFERENCES AND NOTES

1. Xia, T.; Li, N.; Nel, A. E. Potential Health Impact of Nanoparticles. *Annu. Rev. Public Health* **2009**, *30*, 137–150.
2. Lin, Y.; Smith, T. W.; Alexandridis, P. Adsorption of a Polymeric Siloxane Surfactant on Carbon Black Particles Dispersed in Mixtures of Water with Polar Organic Solvents. *J. Colloid Interface Sci.* **2002**, *255*, 1–9.
3. Roller, M. Carcinogenicity of Inhaled Nanoparticles. *Inhal. Toxicol.* **2009**, *21*, 144–157.
4. International Agency for Research on Cancer. Carbon Black, Titanium Dioxide and Talc. *IARC Monogr. Eval. Carcinog. Risks Hum.* 2010, *93*, 43-191.
5. *Carbon Black User's Guide*; International Carbon Black Association: 2006.
6. Wang, Z.; Liu, J.; Wu, S.; Wang, W.; Zhang, L. Novel Percolation Phenomena and Mechanism of Strengthening Elastomers by Nanofillers. *Phys. Chem. Chem. Phys.* **2010**, *12*, 3014–3030.
7. Clayson, D. B. *Toxicological Carcinogenesis.* Lewis Publishers: Boca Raton, FL, 2001.
8. Kim, D.; Guengerich, F. P. Cytochrome P450 Activation of Arylamines and Heterocyclic Amines. *Annu. Rev. Pharmacol. Toxicol.* **2005**, *45*, 27–49.
9. National Toxicology Program. *11th Report on Carcinogens;* U.S. Department of Health and Human Services: Washington, DC, 2005.
10. de Vocht, F.; Sobala, W.; Wilczynska, U.; Kromhout, H.; Szeszenia-Dabrowska, N.; Peplonska, B. Cancer Mortality and Occupational Exposure to Aromatic Amines and Inhalable Aerosols in Rubber Tire Manufacturing in Poland. *Cancer Epidemiol.* **2009**, *33*, 94–102.
11. Cedervall, T.; Lynch, I.; Lindman, S.; Berggard, T.; Thulin, E.; Nilsson, H.; Dawson, K. A.; Linse, S. Understanding the Nanoparticle-Protein Corona Using Methods to Quantify Exchange Rates and Affinities of Proteins for Nanoparticles. *Proc. Natl. Acad. Sci. U.S.A.* **2007**, *104*, 2050–2055.
12. Zhang, B.; Xing, Y.; Li, Z.; Zhou, H.; Mu, Q.; Yan, B. Functionalized Carbon Nanotubes Specifically Bind to α-Chymotrypsin's Catalytic Site and Regulate its Enzymatic Function. *Nano Lett* **2009**, *9*, 2280–2284.
13. Asuri, P.; Karajanagi, S. S.; Vertegel, A. A.; Dordick, J. S.; Kane, R. S. Enhanced Stability of Enzymes Adsorbed onto Nanoparticles. *J. Nanosci. Nanotechnol.* **2007**, *7*, 1675–1678.
14. Chakraborti, S.; Chatterjee, T.; Joshi, P.; Poddar, A.; Bhattacharyya, B.; Singh, S. P.; Gupta, V.; Chakrabarti, P. Structure and Activity of Lysozyme on Binding to ZnO Nanoparticles. *Langmuir* **2010**, *26*, 3506–3513.
15. Chandra, G.; Ghosh, K. S.; Dasgupta, S.; Roy, A. Evidence of Conformational Changes in Adsorbed Lysozyme Molecule on Silver Colloids. *Int. J. Biol. Macromol.* **2010**, *47*, 361–365.
16. Xu, Z.; Liu, X. W.; Ma, Y. S.; Gao, H. W. Interaction of Nano-TiO_2 with Lysozyme: Insights into the Enzyme Toxicity of Nanosized Particles. *Environ. Sci. Pollut. Res. Int.* **2010**, *17*, 798–806.
17. Frohlich, E.; Kueznik, T.; Samberger, C.; Roblegg, E.; Wrighton, C.; Pieber, T. R. Size-Dependent Effects of Nanoparticles on the Activity of Cytochrome P450 Isoenzymes. *Toxicol. Appl. Pharmacol.* **2010**, *242*, 326–332.
18. Lamb, J. G.; Hathaway, L. B.; Munger, M. A.; Raucy, J. L.; Franklin, M. R. Nano-silver Particle Effects on Drug Metabolism *in Vitro*. *Drug Metab. Dispos.* **2010**, *38*, 2246–2251.

19. Dupret, J. M.; Rodrigues-Lima, F. Structure and Regulation of the Drug-Metabolizing Enzymes Arylamine *N*-Acetyltransferases. *Curr. Med. Chem.* **2005**, *12*, 311–318.
20. Hein, D. W. Molecular Genetics and Function of NAT1 and NAT2: Role in Aromatic Amine Metabolism and Carcinogenesis. *Mutat. Res.* **2002**, *506−507*, 65–77.
21. Setyan, A.; Sauvain, J. J.; Rossi, M. J. The Use of Heterogeneous Chemistry for the Characterization of Functional Groups at the Gas/Particle Interface of Soot and TiO_2 Nanoparticles. *Phys. Chem. Chem. Phys.* **2009**, *11*, 6205–6217.
22. L'Azou, B.; Jorly, J.; On, D.; Sellier, E.; Moisan, F.; Fleury-Feith, J.; Cambar, J.; Brochard, P.; Ohayon-Courtes, C. *In Vitro* Effects of Nanoparticles on Renal Cells. *Part. Fibre Toxicol.* **2008**, *5*, 22.
23. Hussain, S.; Thomassen, L. C.; Ferecatu, I.; Borot, M. C.; Andreau, K.; Martens, J. A.; Fleury, J.; Baeza-Squiban, A.; Marano, F.; Boland, S. Carbon Black and Titanium Dioxide Nanoparticles Elicit Distinct Apoptotic Pathways in Bronchial Epithelial Cells. *Part Fibre Toxicol.* **2010**, *7*, 10.
24. Hussain, S.; Boland, S.; Baeza-Squiban, A.; Hamel, R.; Thomassen, L. C.; Martens, J. A.; Billon-Galland, M. A.; Fleury-Feith, J.; Moisan, F.; Pairon, J. C.; Marano, F. Oxidative Stress and Proinflammatory Effects of Carbon Black and Titanium Dioxide Nanoparticles: Role of Particle Surface Area and Internalized Amount. *Toxicology* **2009**, *260*, 142–149.
25. Dimova, S.; Hoet, P. H.; Nemery, B. Xenobiotic-Metabolizing Enzyme Activities in Primary Cultures of Rat Type II Pneumocytes and Alveolar Macrophages. *Drug Metab. Dispos.* **2001**, *29*, 1349–1354.
26. Kulaksiz, H.; Schmid, A.; Honscheid, M.; Ramaswamy, A.; Cetin, Y. Clara Cell Impact in Air-Side Activation of CFTR in Small Pulmonary Airways. *Proc. Natl. Acad. Sci. U.S.A.* **2002**, *99*, 6796–6801.
27. Castell, J. V.; Donato, M. T.; Gomez-Lechon, M. J. Metabolism and Bioactivation of Toxicants in the Lung. The *in Vitro* Cellular Approach. *Exp. Toxicol. Pathol.* **2005**, *57*, 189–204.
28. Clouter, A.; Richards, R. J. Extracellular Biotransformation Potential in Mouse Airways. *Int. J. Biochem. Cell Biol.* **1997**, *29*, 521–527.
29. Dairou, J.; Petit, E.; Ragunathan, N.; Baeza-Squiban, A.; Marano, F.; Dupret, J. M.; Rodrigues-Lima, F. Arylamine *N*-Acetyltransferase Activity in Bronchial Epithelial Cells and Its Inhibition by Cellular Oxidants. *Toxicol. Appl. Pharmacol.* **2009**, *236*, 366–371.
30. Sauvain, J. J.; Deslarzes, S.; Riediker, M. Nanoparticle Reactivity toward Dithiothreitol. *Nanotoxicology* **2008**, *2*, 121–129.
31. Rodrigues-Lima, F.; Dupret, J. M. Regulation of the Activity of the Human Drug Metabolizing Enzyme Arylamine *N*-Acetyltransferase 1: Role of Genetic and Nongenetic Factors. *Curr Pharm Des* **2004**, *10*, 2519–2524.
32. Dairou, J.; Atmane, N.; Rodrigues-Lima, F.; Dupret, J. M. Peroxynitrite Irreversibly Inactivates the Human Xenobiotic-Metabolizing Enzyme Arylamine *N*-Acetyltransferase 1 (NAT1) in Human Breast Cancer Cells: A Cellular and Mechanistic Study. *J. Biol. Chem.* **2004**, *279*, 7708–7714.
33. Sreerama, N.; Venyaminov, S. Y.; Woody, R. W. Estimation of Protein Secondary Structure from Circular Dichroism Spectra: Inclusion of Denatured Proteins with Native Proteins in the Analysis. *Anal. Biochem.* **2000**, *287*, 243–251.
34. Magdaleno, S. M.; Wang, G.; Jackson, K. J.; Ray, M. K.; Welty, S.; Costa, R. H.; DeMayo, F. J. Interferon-Gamma Regulation of Clara Cell Gene Expression: *In Vivo* and *In Vitro*. *Am. J. Physiol.* **1997**, *272*, L1142–1151.
35. Grant, D. M.; Blum, M.; Beer, M.; Meyer, U. A. Monomorphic and Polymorphic Human Arylamine *N*-Acetyltransferases: A Comparison of Liver Isozymes and Expressed Products of Two Cloned Genes. *Mol. Pharmacol.* **1991**, *39*, 184–191.
36. Wu, H. C.; Lu, H. F.; Hung, C. F.; Chung, J. G. Inhibition by Vitamin C of DNA Adduct Formation and Arylamine *N*-Acetyltransferase Activity in Human Bladder Tumor Cells. *Urol. Res.* **2000**, *28*, 235–240.